

The Development of Three-dimensional Wall Jet

H. Sun

Ph. D Candidate

McMaster University, ON, Canada

(905)5259140-22007

email:sunh@mcmail.cis.mcmaster.ca

D. Ewing

Assistant Professor

McMaster University, ON, Canada

(905)5259140-27476

email: ewingd@mcmaster.ca

Abstract

Detailed flow field measurements were performed in the near and intermediate field of the three-dimensional wall jet exiting a round jet. It was found that the profiles of the mean streamwise and lateral velocity are approximately self-similar in the region $25 \leq x/D \leq 40$. The profiles of the turbulent Reynolds stresses required longer to become self-similar, as expected, but seem to be self-similar by $x/D \approx 40$. The mean streamwise vorticity contours on cross-stream planes in the wall jet also changed until $x/D \approx 40$ indicating that the large-scale structures that contribute to these measurements are still evolving to this point in the flow. The change in the orientation of the two regions of counter rotating vorticity on each side of the jet centreline in the region $15 \leq x/D \leq 40$ can be used to explain the change in the jets lateral growth rate observed in this region.

Introduction

The three-dimensional wall jet formed by a round jet exiting over a flat plate is an useful model of the wall jets used in many film cooling applications. One feature of wall jets that makes them useful for film cooling is that they have large lateral growth rates. This large lateral growth rate and the streamline curvature associated with it makes these flows challenging to predict using turbulent models. There is interest in using the three-dimensional wall jet formed by a round jet as a test case for turbulence models because it includes these features in a flow with a relatively simple geometry. There have been a number of investigations that presented detailed measurements in the far field of this wall jet (e.g. Abrahamsson et al. [1]) but far fewer have presented detail measurements in the near and intermediate field.

Davis and Winarto [3] reported measurements of the mean velocity and turbulent Reynolds stress profiles in the region $x/D \leq 64$, where x is the distance downstream of the jet nozzle and D the jet diameter. Iida and Matsuda [6] reported mean streamwise vorticity contours measured in the near field, $0 \leq x/D \leq 16$, where the large lateral growth of the jet is initiated. Matsuda et al. [7] and Ewing and Pollard [4] performed more detailed measurements of the large-scale structures in this region. They proposed that structures consisting of a pair of horse-shoe vortices form in the near field causing the large lateral spreading of the jet.

Davis and Winarto [3] found that the lateral growth rate of the jet continued to increase until $x/D \approx 40$. After this location the growth rate of the wall jet was approximately constant and the profiles of the

mean velocity and turbulent stresses were self-similar. However, Davis and Winarto [3] only reported measurements on a single plane between $x/D=16$ and 48 and did not explain why the lateral growth rate of the jet continued to change in this region.

The objective of this investigation was to perform detailed measurements in the intermediate region of the wall jet, $20 \leq x/D \leq 40$, and to examine why the growth rate of the jet continues to change through this region. The profiles of the mean velocities and turbulent Reynolds stresses were measured on planes every 5 diameters downstream of the jet. The profiles were scaled using the predictions of the similarity analysis outlined recently by Sun and Ewing [8] in order to examine how the flow evolves to its final self-similar state. The three-dimensional development of the wall jet was also examined by measuring the distribution of the mean velocity and mean streamwise vorticity on the downstream-stream planes. The measurements in the intermediate region are compared with measurements from the near field.

Self-Similar Solutions

There have been a number of investigations that have shown that the mean velocity and turbulent stress profiles are self-similar in the far field of the three-dimensional wall jet shown in figure 1 (e.g. Abrahamsson et al. [1]). Sun and Ewing [8] recently demonstrated that the first order governing equations in this region have self-similar solutions. The predictions from this analysis are used here to scale the profiles of mean velocities and turbulent stresses so the methodology and results are outlined before the measurements are presented.

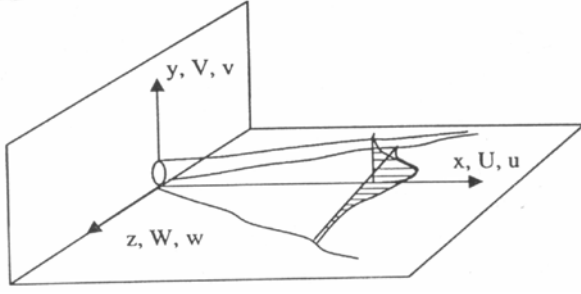


Figure 1: Schematic of the three-dimensional wall jet

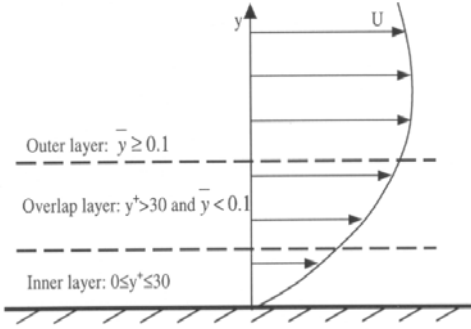


Figure 2: Sketch of the two layers in the wall jet.

Following the approach outlined by George et al. [5] for the two-dimensional wall jet, the high-Reynolds-number three-dimensional wall jet can be separated into two layers shown in figure 2. An outer layer where the viscous stresses are negligible and an inner layer where the mean convection is negligible. The first order solutions from these two layers must match in the overlap layer between the two layers.

The Reynolds averaged governing equations for the outer layer can be simplified by recognizing that the length scale in the lateral direction is much larger than the length scale in vertical direction. Utilizing this assumption with the standard thin-shear-layer and large Reynolds number assumptions it can be shown the first-order mean momentum equation in the outer layer are given by

$$U \frac{\partial U}{\partial x} + V \frac{\partial U}{\partial y} + W \frac{\partial U}{\partial z} = -\frac{\partial \bar{uv}}{\partial y}, \quad (1)$$

and

$$U \frac{\partial W}{\partial x} + V \frac{\partial W}{\partial y} + W \frac{\partial W}{\partial z} = -\frac{\partial \bar{vw}}{\partial y}, \quad (2)$$

where U, V, W and u, v, w are the mean and fluctuating velocities in the streamwise, x , vertical, y , and lateral direction, z , shown in figure 1.

| Self-similar Solution | Constraint |
|--|--|
| $U = U_{s,o}(x)f_{U,o}(\bar{y}, \bar{z})$ | $U_{s,o} = U_{\max}$ |
| $V = V_o(x)f_{V,o}(\bar{y}, \bar{z})$ | $V_o \propto U_{s,o} dy_{1/2} / dx$ |
| $W = W_o(x)f_{W,o}(\bar{y}, \bar{z})$ | $W_o \propto U_{s,o} dz_{1/2} / dx$ |
| $\Omega_x = \Omega_o(x)f_{\Omega,o}(\bar{y}, \bar{z})$ | $\Omega_o \propto (U_{s,o} dz_{1/2} / dx) / y_{1/2}$ |
| $\bar{uv} = R_{uv,o}(x)f_{uv,o}(\bar{y}, \bar{z})$ | $R_{uv,o} \propto U_{s,o}^2 dy_{1/2} / dx$ |
| $\bar{vw} = R_{vw,o}(x)f_{vw,o}(\bar{y}, \bar{z})$ | $R_{vw,o} \propto U_{s,o} W_o dy_{1/2} / dx$ |
| $\bar{uw} = R_{uw,o}(x)f_{uw,o}(\bar{y}, \bar{z})$ | $R_{uw,o} \propto U_{s,o}^2 dz_{1/2} / dx$ |
| $\bar{u}^2 = k_{u,o}(x)f_{u,o}(\bar{y}, \bar{z})$ | $k_{u,o} \propto U_{s,o}^2$ |
| $\bar{v}^2 = K_{v,o}(x)f_{v,o}(\bar{y}, \bar{z})$ | $k_{v,o} \propto U_{s,o}^2$ |
| $\bar{w}^2 = K_{w,o}(x)f_{w,o}(\bar{y}, \bar{z})$ | $k_{w,o} \propto U_{s,o}^2$ |

Table 1: Similarity solutions in outer layer

Following George et al. [5], it is proposed that the mean velocities and turbulent stresses in the momentum equations have self-similar solution of form given in table 1. Here, $\bar{y} = y / y_{1/2}$ and $\bar{z} = z / z_{1/2}$ are the vertical and lateral coordinate normalized by the half-widths of the jet, $y_{1/2}$ and $z_{1/2}$. Substituting these solutions into the mean streamwise momentum equation yields

$$\begin{aligned} & [U_{s,o} \frac{dU_{s,o}}{dx}] f_{U,o} - [\frac{U_{s,o}^2}{y_{1/2}} \frac{dy_{1/2}}{dx}] \frac{\partial f_{U,o}}{\partial \bar{y}} \bar{y} \\ & - [\frac{U_{s,o}^2}{z_{1/2}} \frac{dz_{1/2}}{dx}] \frac{\partial f_{U,o}}{\partial \bar{z}} \bar{y} + [\frac{V_o U_{s,o}}{y_{1/2}}] \frac{\partial f_{U,o}}{\partial \bar{y}} f_V \\ & + [\frac{W_o U_{s,o}}{z_{1/2}}] \frac{\partial f_{U,o}}{\partial \bar{z}} f_W = -[\frac{R_{uv,o}}{y_{1/2}}] \frac{\partial f_{uv,o}}{\partial \bar{y}}. \quad (3) \end{aligned}$$

It follows that the proposed self-similar solutions are consistent with this equation if the terms in square bracket are proportional. Applying the same approach to the lateral momentum equation and the first order equations for the turbulent Reynolds stresses it follows that these equations have self-similar solutions if the constraints outlined in table 1 are satisfied.

There are two different velocity scales in the flow if the lateral growth rate is not constant. The analysis of the governing equations does not impose any constraints on the growth rate of either length scale in the flow but if the growth rate of either increases with downstream position the dominant production terms in the turbulent kinetic energy equations are different than if the growth rate is constant or decreases. Thus, there is a difference in the underlying flow physics for these different cases.

| Self-similar Solution | Constraint |
|---|-----------------------------|
| $U = U_{s,i}(x)f_{U,i}(y^+, \bar{z})$ | $U_{s,i}(x) \propto u_*$ |
| $W = W_i(x)f_{W,i}(y^+, \bar{z})$ | $W_i(x) \propto w_*$ |
| $\overline{uv} = R_{uv,i}(x)f_{uv,i}(y^+, \bar{z})$ | $R_{uv,i}(x) \propto u_*^2$ |
| $\overline{vw} = R_{vw,i}(x)f_{vw,i}(y^+, \bar{z})$ | $R_{vw,i}(x) \propto w_*^2$ |

Table 2: Similarity solutions in inner layer

It follows that the solution for the mean streamwise vorticity is given by

$$\begin{aligned} \Omega_x &= \frac{\partial W}{\partial y} - \frac{\partial V}{\partial z} \\ &= \left[\frac{W_o}{y_{1/2}} \right] \frac{\partial f_{W,o}}{\partial y} - \left[\frac{V_o}{z_{1/2}} \right] \frac{\partial f_{V,o}}{\partial z}. \end{aligned} \quad (4)$$

The size of the two scales in this equation depend on the x-dependence of the two length and velocity scales. It is assumed here that the first term in equation (4) makes the dominant contribution to the streamwise vorticity, which is true in the intermediate field, so the scale for this term is used for the mean streamwise vorticity.

Using the boundary-layer assumptions it is straightforward to show that the first-order momentum equations in the inner layer are given by

$$\frac{\tau_{w,x}}{\rho} = u_*^2 = -\overline{uv} + \nu \frac{\partial U}{\partial y}, \quad (5)$$

and

$$\frac{\tau_{w,z}}{\rho} = w_*^2 = -\overline{vw} + \nu \frac{\partial W}{\partial y}, \quad (6)$$

where $\tau_{w,x}$ and $\tau_{w,z}$ and the mean wall shear stress in streamwise and lateral direction, respectively. Here, u_* and w_* are the friction velocity in the streamwise and lateral direction. It is proposed that the profiles of the mean velocity and turbulent stresses in these equations have solutions of the form given in table 2, where $y^+ = y/\eta$ and $\eta = \nu/U_{s,i}$. Substituting these solutions into equations (5) and (6), it is straightforward to show these equations have similarity solutions if the constraints in table 2 are satisfied. The analysis can also be extended to the Reynolds stress equations in the inner layer.

The friction laws for the three-dimensional wall jet can be determined by matching the solutions in the overlap layer, where the turbulent shear stresses \overline{uv} and \overline{vw} are constant to first order. In this case, the similarity scales for these moments in the inner

and outer layers must be proportional. Thus, the skin friction coefficient is given by

$$c_{f,x} = \frac{u_*^2}{U_{\max}^2} \propto \frac{dy_{1/2}}{dx}, \quad (7)$$

and the ratio of two friction velocities is given by

$$\frac{w_*}{u_*} \propto \sqrt{\frac{dz_{1/2}}{dx}}. \quad (8)$$

The Reynolds number of the jet also decreases as the flow evolves downstream so that the skin friction would increase with Reynolds number if the growth rate of the flow is constant or decreases with downstream position.

Experimental Facility and Procedure

The wall jet studied here is formed by a round jet exiting a contoured nozzle with a diameter of 3.8 cm. The contour of nozzle is a fifth order polynomial and the area contraction in the nozzle is 28:1. The flow enters the nozzle from a 20 cm diameter pipe that contains both a honeycomb and screens for flow conditioning. The air flow into the pipe is supplied from a large settling chamber with foam barriers, honeycomb and screens through a bell-mouth. The flow through the system is driven by a 1/2 HP blower. The exit velocity for the measurements reported here was 45 m/s, which corresponds to a Reynolds number of 108,000. The exit profile was uniform to within 1.0% and the turbulence intensity at the exit was less than 0.25%.

The jet exiting the contoured nozzle flows out over a horizontal plate with a length of 48 outlet diameters (D) and a width of 64 diameters. Previous studies have shown this plate is sufficiently wide to ensure the development of wall jet is not affected by the edges of the plate. A plate, with a height of 32 D and a width of 64 D, is mounted flush with the nozzle outlet to prevent entrainment from behind the nozzle.

The velocity field in the wall jet was measured using hot-wire anemometry. The hot-wire transducers were moved through the flow using a three-dimensional traverse. The traverse is moved in the vertical and lateral direction using stepper motors that can move the transducer in steps of approximately 0.04 mm. The probe was moved manually in the streamwise direction. The mean velocity and turbulent stresses were measured along the centreline of the wall jet and laterally across the jet at the height coinciding to the maximum velocity point on the centreline for positions ranging from $x/D=3$ to $x/D=40$ using single and cross-wire probes. Boundary layer probes were used for the near wall measurements.

The single wire probes were calibrated by fitting a fourth order polynomial to approximately 20 points. The cross wire probes were calibrated following a similar procedure for each wire and then determining

the angular sensitivity of the wires [2]. The ambient temperature changed by less than 1°C and the measurements were corrected for changes in the temperature. The uncertainty in the measurements of the mean velocity and turbulence stresses shown in the profiles is 2% and 9% respectively. The uncertainty in the mean velocity measurements used to generate the contour plots is approximately 4%. The cross-flow error in the measurements of the mean velocities, U and W , is 3-4% at the half-velocity points in the flow and 10-12% in measurements of the turbulent Reynolds stresses at these points.

Experimental Results

The development of the wall jet was measured in both near and intermediate region of the jet. Initially, the development of the jet was characterized by examining the evolution of the length and velocity scales of the jet. The spread of the wall jet in the vertical and lateral direction was characterized by the half widths shown in figure 3. The vertical half-width $y_{1/2}$ is the distance along the centreline from the wall to the outside point where the velocity is half of the local maximum velocity. The lateral half-width $z_{1/2}$ is the lateral distance between maximum velocity point on the centreline of the jet to the point at the same height where the velocity is half of the maximum velocity. The growth rate of the vertical length scale in the region $20 \leq x/D \leq 40$ is 0.045, which falls between the values reported by Abrahamsson et al. [1], 0.065, and Davis and Winarto [3], 0.037 for wall jets exiting contoured nozzles. The measurements of the lateral half-width are in good agreement with the data reported by Davis and Winarto [3]. It is evident that the lateral growth rate of the jet increases in the region $20 \leq x/D \leq 40$ as Davis and Winarto reported.

The maximum mean streamwise velocity measured in the wall jet normalized by the outlet velocity is shown in figure 4. The local maximum velocity is approximately constant before $x/D=6$, which corresponds to the end of the potential core in a free jet. The mean velocity then rapidly decays as the flow evolves downstream causing the Reynolds number of the flow to decrease as it evolves downstream.

The ratio of the local maximum lateral mean velocity to the local maximum mean streamwise velocity is shown in figure 5. This ratio is changing throughout the intermediate region indicating there are two different velocity scales in this region of the flow. This is not unexpected since the similarity analysis predicted there should be two velocity scales in the flow when the lateral growth rate was changing.

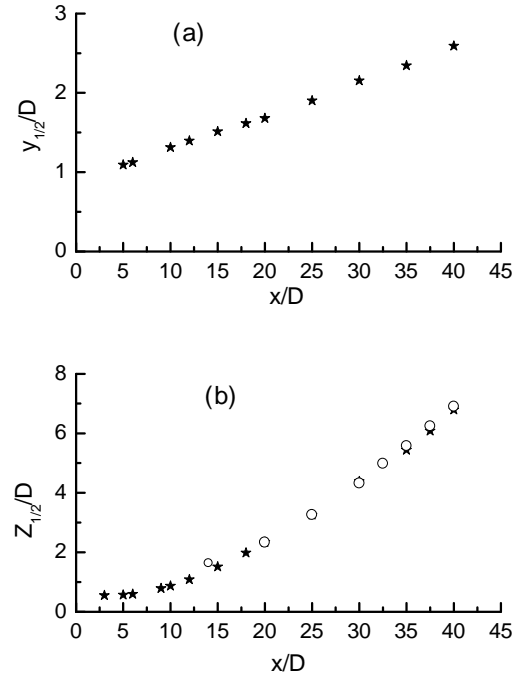


Figure 3: The development of jet half-width in (a) vertical, (b) lateral direction measured \star here and \circ by Davis and Winarto[3].

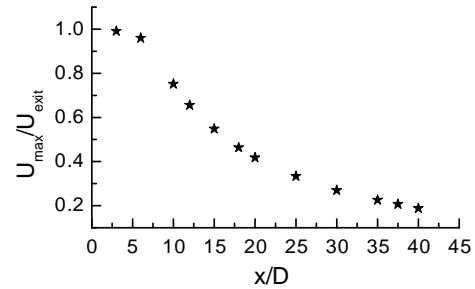


Figure 4: The decay of the maximum velocity

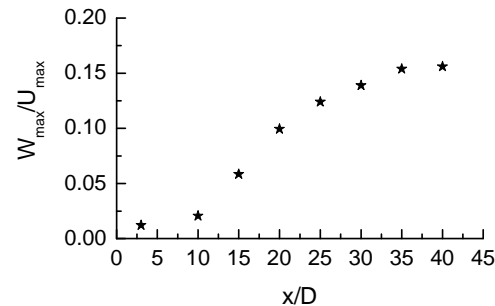


Figure 5: The ratio of the mean streamwise and lateral velocity

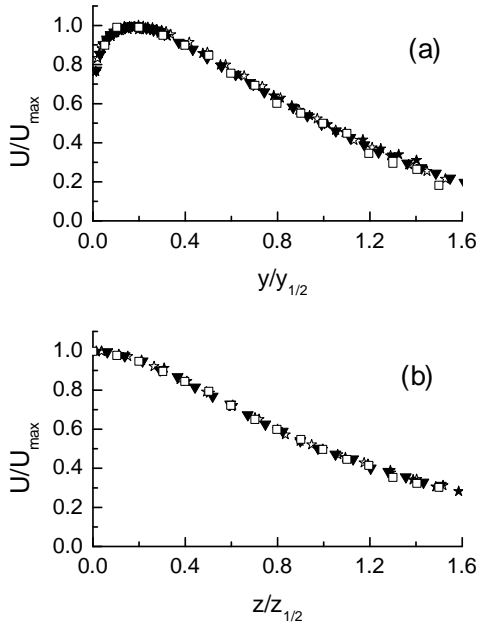


Figure 6: Profiles of the mean streamwise velocity in (a) vertical direction, (b) lateral direction measured at $\star x/D=20$, $\blacktriangledown x/D=30$, $\star x/D=40$ and $\square 50 \leq x/D \leq 90$ reported by Abrahamsson et al. [1].

The profiles of the mean streamwise velocity measured in the vertical direction along the centreline of the wall jet in the region $20 \leq x/D \leq 40$ are shown in figure 6 (a), while the profiles measured in the lateral direction at the height of the maximum velocity in the same region are shown in figure 6(b). The mean velocity has been normalized by the local maximum velocity and the coordinates normalized by the local half width. It is clear that the measured profiles in the entire region collapse when scaled in the manner predicted in the similarity analysis. The profiles are also in good agreement with the self-similar profile reported by Abrahamsson et al. [1] for the far field of the wall jet.

The profiles of the mean lateral velocity across the jet are shown in figure 7. The velocities have been scaled using the local velocity scale predicted in the similarity analysis rather than U_{\max} that is traditionally used. It is clear that the profiles of the lateral mean velocity collapse reasonably well beyond $x/D=25$ when they are scaled using the velocity scale predicted in the similarity analysis. Thus, there are two different characteristic velocity scales in the intermediate region of the flow.

It is useful to examine the development of the turbulent Reynolds stresses in order to determine how the turbulent processes in the wall jet are evolving to their equilibrium state. The profiles of the turbulence

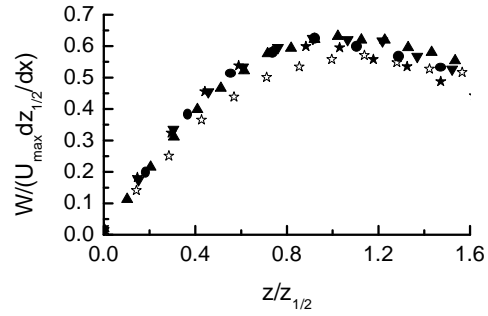


Figure 7: Profiles of mean lateral velocity measured at $\star x/D=20$, $\blacktriangle x/D=25$, $\blacktriangledown x/D=30$, $\bullet x/D=35$, and $\star x/D=40$.

intensities, u' , v' , and w' measured in the intermediate field of the wall jet are shown in figures 8-10. The turbulence intensities have been scaled using the local maximum mean velocity, the velocity scale predicted in the similarity analysis. The vertical and lateral profiles have been measured in the same positions as the mean velocity profiles. Profiles of the turbulence intensity v' in the lateral direction were not measured because it is difficult to measure this moment accurately using hot-wire anemometry across the jet because the mean lateral velocity is large.

It is clear that the profiles of the turbulence intensities take longer to become self-similar, as expected. The profiles are uniformly approaching a self-similar profile and seem to become approximately self-similar at $x/D \approx 35$. The profiles measured at this location are in good agreement with the self-similar profile for the far field of the wall jet reported by Abrahamsson et al. [1].

The profiles of the Reynolds shear stresses measured in the wall jet are shown in figure 11 and 12. The vertical profiles of the shear stress \overline{uw} collapse in the intermediate field when scaled in the manner predicted by the similarity analysis. This is not unexpected since this Reynolds stress is the dominant transfer mechanism for mean streamwise momentum in the outer region of the wall jet. The lateral profile of this moment was not measured.

The profiles of \overline{uw} do not collapse when they are scaled in the manner predicted in the similarity analysis but do collapse when they are scaled using U_{\max}^2 . This result suggests that the mechanism causing the large lateral spreading has not yet developed to its final equilibrium or there is another set of self-similar solutions that were not considered in the analysis. The first possibility was considered here by performing measurements of the three-dimensional development of the velocity field.

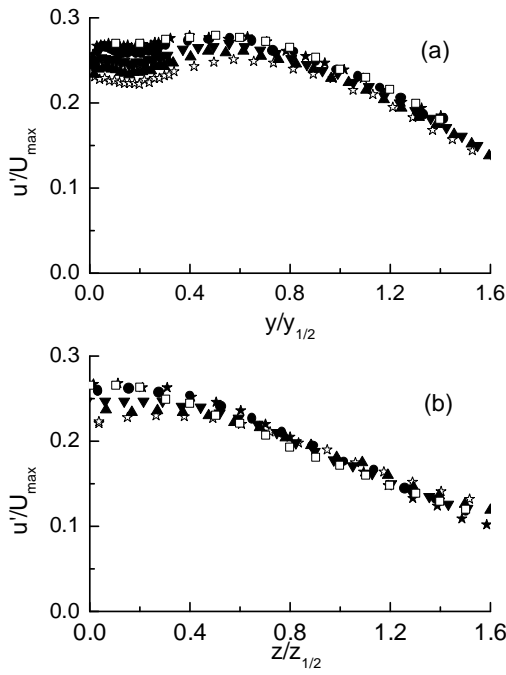


Figure 8: Profiles of streamwise turbulence intensity in (a) vertical direction, (b) lateral direction measured at $\star x/D=20$, $\blacktriangledown x/D=30$, $\bullet x/D=35$, $\star x/D=40$ and $\square 50 \leq x/D \leq 90$ reported by Abrahamsson et al. [1].

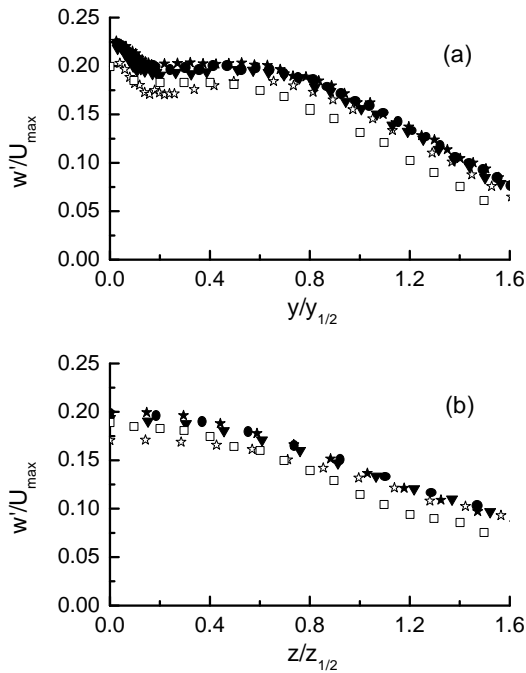


Figure 9: Profiles of lateral turbulence intensity in (a) vertical direction, (b) lateral direction measured at $\star x/D=20$, $\blacktriangledown x/D=30$, $\bullet x/D=35$, $\star x/D=40$ and $\square 50 \leq x/D \leq 90$ reported by Abrahamsson et al. [1].

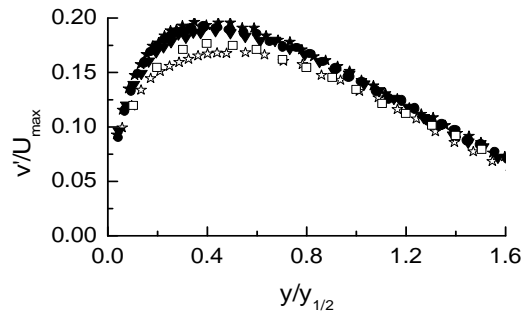


Figure 10: Profiles of vertical turbulence intensity in vertical direction measured at $\star x/D=20$, $\blacktriangledown x/D=30$, $\bullet x/D=35$, $\star x/D=40$, and $\square 50 \leq x/D \leq 90$ reported by Abrahamsson et al. [1].

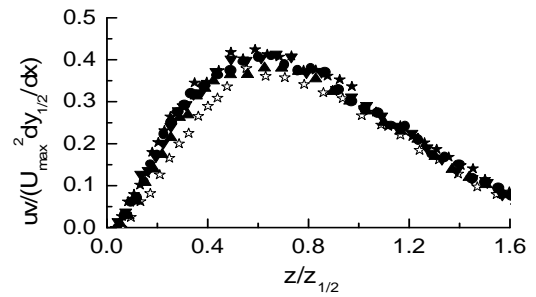


Figure 11: Profiles of shear stress \overline{uw} measured at $\star x/D=20$, $\blacktriangle x/D=25$, $\blacktriangledown x/D=30$, $\bullet x/D=35$, and $\star x/D=40$.

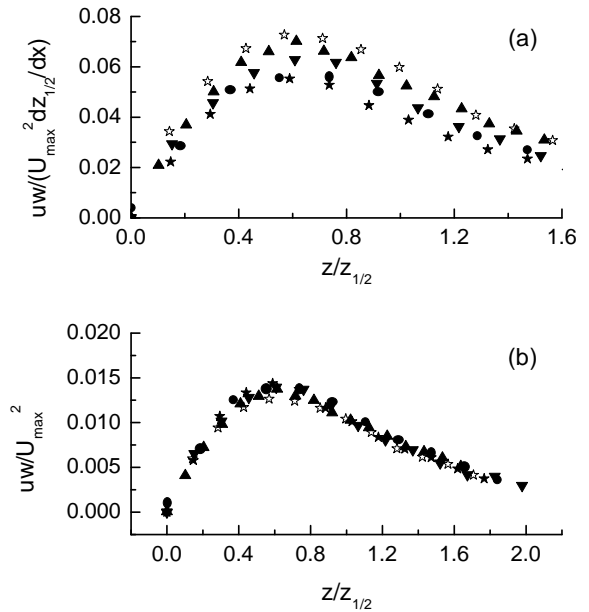


Figure 12: Profiles of shear stress \overline{uw} normalized by (a) $U_{\max}^2 dz_{1/2}/dx$, (b) U_{\max}^2 measured at $\star x/D=20$, $\blacktriangle x/D=25$, $\blacktriangledown x/D=30$, $\bullet x/D=35$, and $\star x/D=40$.

The three-dimensional development of the velocity field was examined by measuring the distribution of the mean velocity on cross-stream planes downstream of the jet exit. The contours of the mean streamwise velocity normalized by the local maximum velocity at $x/D=6, 15, 20$ and 30 are shown in figure 13. The dotted line on these contour plots indicates the height of the maximum velocity point. The height of this point decreases as the flow evolves downstream until it reaches $x/D \approx 20$ after which it increases. It is also clear that the height of the maximum velocity point and the maximum jet width, shown by the solid lines in the plots, do not coincide in the near field. Initially the jet spreads laterally near the wall so that the height of the maximum jet width is below the height of the maximum velocity point. The height of the maximum width increases until it roughly coincides with the height of the maximum velocity point at $x/D \approx 20-25$. Beyond the point the two heights roughly coincide and both increase.

The distribution of the mean lateral velocity was also measured on a number of downstream planes. The profiles in the vertical direction were measured with a small spacing so they could be used to estimate the mean streamwise vorticity; i.e.,

$$\Omega_x \approx \frac{\partial W}{\partial y} \quad (9)$$

The contours of the mean streamwise vorticity normalized by $(U_{\max} dz_{1/2} / dx) / y_{1/2}$, the scale deduced in the similarity analysis, at $x/D=15, 25, 35$, and 40 are shown in figure 14. The broken and solid lines indicate clockwise and counter clockwise motions viewed from the nozzle. The mean vorticity contours continue to change as the flow evolves downstream indicating that the large-scale structures that contribute to these measurements are changing. In particular, the outer vortex induces the inner streamwise vortex below it until they are positioned roughly one over the other. This repositioning of the vortices would cause the induced motion caused by the two vortices to become parallel to the wall likely explaining why the lateral growth rate of the flows increases over this region. The magnitude of the scaled vorticity decreases as flow evolves downstream and becomes approximately constant by $x/D=35-40$.

Summary and Conclusions

Detailed measurements have been performed in the near and intermediate region of the three-dimensional wall jet formed by a round jet. The profiles of the mean streamwise and mean lateral velocity were approximately self-similar in the intermediate field when they were scaled in the manner predicted by the similarity analysis outlined by

Sun and Ewing[7]. The profiles of the turbulent intensities take longer to become self-similar but seem to collapse beyond $x/D > 35$, with the exception of the shear stress \overline{uw} . Further investigation is required to explain why this moment requires so long to collapse.

The measurements of the mean velocity and vorticity distribution on the downstream planes showed that the development of the wall jet is three-dimensional. The height of the largest jet width moves away from the wall as the flow develops while the position of the maximum velocity moves toward the wall until $x/D \approx 20-25$. The height of these two locations roughly coincides beyond this point and move away from the wall. The contours of the mean streamwise vorticity continue to change as the flow evolves downstream until $x/D \approx 35$ indicating the large-scale motions are changing and causing an induced motion more parallel to the wall as the flow evolves downstream.

Acknowledgements

The authors would like to acknowledge the support of NSERC.

References

- [1] Abrahamsson, H., Johansson, B. and Lofdahl, L., 1997, "The turbulence field of a fully developed three-dimensional wall jet", *Internal Report 97/1*, Department of thermo and fluid dynamics, Chalmers University of Technology, Sweden.
- [2] Champagne, H., Sleicher, C. A., and Wehrmann, O. H., 1966, "Turbulence measurements with inclined hot-wires. Part 1: Heat transfer experiments with inclined hot-wire", *J. Fluid Mech.*, Vol. 28, pp. 153-175.
- [3] Davis, M. R. and Winarto, H., 1980, "Jet diffusion from a circular nozzle above a solid plane," *J. Fluid Mech.*, Vol. 101, pp. 201-221.
- [4] Ewing, D., and Pollard, A., 1997, "Evolution of the large scale motions in a three-dimensional wall jet," 28th AIAA fluids conference, Snowmass, CO, *Paper AIAA-97*.
- [5] George, W. K., Abrahamsson, H., Eriksson, J., Lofdahl, L. and Karlsson, R.I., 1997, "A similarity theory for the plane wall jet," *Internal Report 97/7*, Department of thermo and fluid dynamics, Chalmers University of Technology, Sweden.
- [6] Iida, S., and Matsuda, H., 1988, "An experimental study of circular turbulent wall jet along a convex wall," *Transaction of Jpn. Soc. Mech. Eng.*, series B, Vol. 54, No. 498, pp. 354-360.
- [7] Matsuda, H., Iida, S. and Hayakawa, M., 1990, "Coherent structures in three-dimensional wall jet," *J. Fluids Eng.*, Vol. 112, pp. 462-467.
- [8] Sun, H. and Ewing, D., June 1999, "Self-similar solutions in a three-dimensional wall jet," *Proceedings of 8th CANCAM Conference*, Hamilton, Canada.

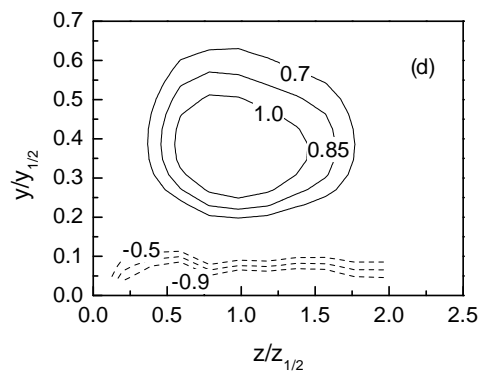
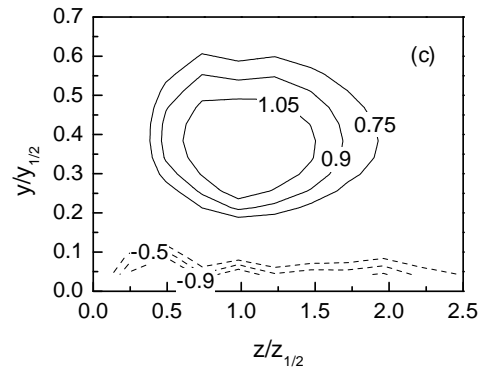
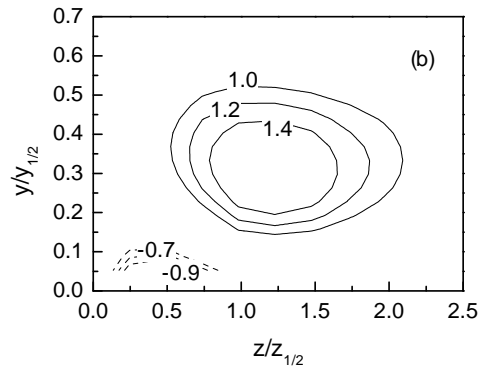
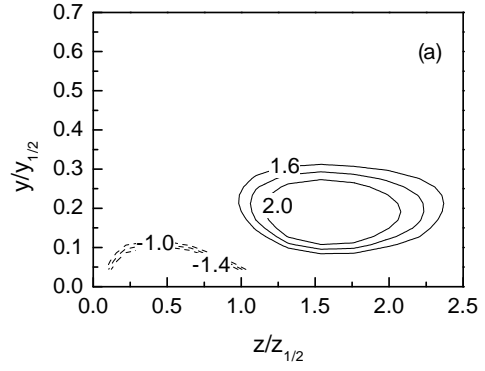
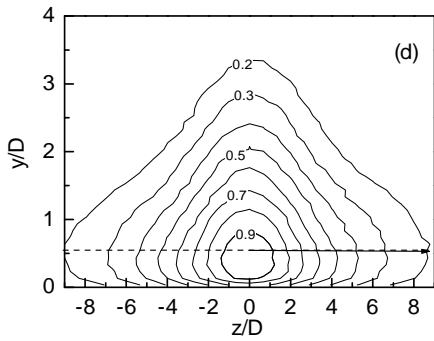
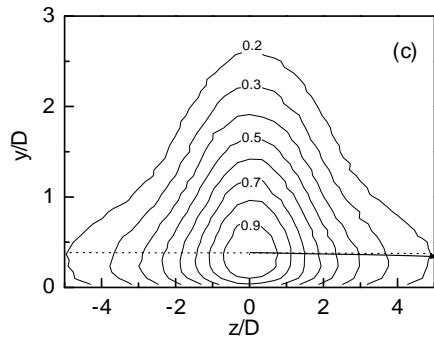
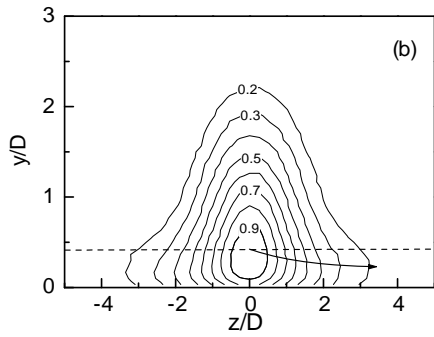
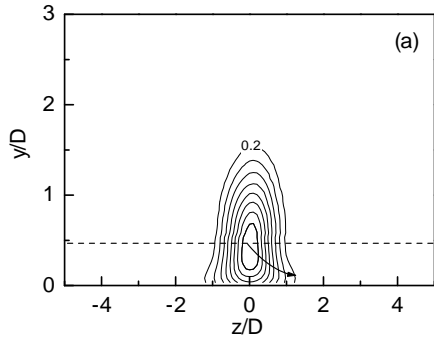


Figure 13: Contours of mean streamwise velocity measured at (a) $x/D=6$, (b) $x/D=15$, (c) $x/D=20$, and (d) $x/D=30$.

Figure 14: Contours of normalized mean streamwise vorticity measured at (a) $x/D=15$, (b) $x/D=25$, (c) $x/D=35$, and (d) $x/D=40$.